Formation of Thermally Induced Craze and Prevention by Using Infrared Radiation Annealing Method

Seong Yun Kim, Sung Ho Kim, Seong Yeol Pak, Jae Ryoun Youn

Department of Materials Science and Engineering, Research Institute of Advanced Materials (RIAM), Seoul National University, Sillim-Dong, Gwanak-Gu, Seoul 151-742, Korea

Received 21 July 2011; accepted 12 October 2011
DOI 10.1002/app.36351
Published online 1 February 2012 in Wiley Online Library (wileyonlinelibrary.com).

ABSTRACT: It is important to study the residual stress distribution and craze formation of transparent overmolded polymeric parts, because the overmolding can cause stress concentration near the interface region and the craze can be generated by the concentrated stress. Thermally induced crazing of an electric appliances product overmolded by using a transparent polymer is discussed in this study. Craze criterion was determined to be 20 MPa at the temperature higher than 60°C by using mechanical characteristic analysis of the polymeric material. Crazes were observed in the product annealed at over 60°C due to thermal residual stresses generated by the temperature difference between the surface and inside of the part upon surface heating. However, they were not observed in the product annealed by infrared radiation (IR) at over 60°C due to simultaneous heating throughout the thickness of the product. The numerical residual stress results were in good agreement with the experimental results, indicating that overmolding process, thermoviscoelastic stress development of the polymeric part, and IR annealing process were considered properly in the three-dimensional numerical analysis. © 2012 Wiley Periodicals, Inc. J Appl Polym Sci 125: 3029–3037, 2012

Key words: crazing; injection molding; simulations; annealing; stress

INTRODUCTION

Residual stresses are generally developed in an injection-molded product. They are caused by a number of reasons, for example, flow-induced residual stresses generated as a result of shear and extensional flows during processing,[1] packing stresses resulting from the high pressure imposed during packing, and thermal stresses developed during solidification and cooling.[3–8] The injection-molded products experience postdeformation due to the residual stresses and viscoelastic property of polymer materials after ejection. Fatal product defects can be generated at high service temperature, because viscoelastic property of the polymeric part is dependent on the temperature according to the time-temperature superposition principle.[9]

Overmolding is an injection molding method that fabricates the product through two time sequential injection molding by using two different polymeric materials in order to improve surface quality and functional characteristics of the injection-molded products and to protect printed matters.[10] The overmolding process may cause severe residual stresses in the product, because heat transfer in the perpendicular direction to the mold wall is asymmetric due to two shots. The severe residual stresses can cause warpage, buckling, and crazes or cracks of the products.[12–15] Also, the postdeformation of the overmolded product can cause the stress concentration and crazing near the interface between the two different polymeric materials. Especially, the crazes that are not fatal in the aspect of mechanical property of the product can be a serious problem in the case that transparent polymer materials such as polystyrene, polymethylmethacrylate, and polycarbonate (PC) are used as raw materials. Therefore, it is important to investigate the residual stress distribution and craze formation that is one of the most significant problems for practical application of transparent polymeric parts.

Thermal annealing is normally used for lowering residual stresses of the injection-molded products as high temperature is applied to the injection-molded products. However, there is a possibility that effects of the thermal annealing can be reduced because thermal residual stresses occur again due to the temperature difference between surface and inside of the product upon surface heating and low thermal conductivity of polymers.[16] In contrast, infrared (IR)

Correspondence to: J. R. Youn (jaeryoun@snu.ac.kr).
Contract grant sponsor: Ministry of Education, Science and Technology [Basic Science Research Program through the National Research Foundation of Korea (NRF)]; contract grant number: R11-2005-065

annealing can prevent the problem of surface heating caused by the temperature difference between surface and inside of the product, because IR annealing is a bulk heating method by applying electromagnetic energy from IR emitter and can heat every position almost simultaneously.[16] Since residual stresses in overmolded products can be increased due to the stress concentration near the interface between the different polymer materials during annealing, the IR annealing is more appropriate than the surface heating for the overmolded products by using transparent polymer materials.

Craze failure of a TV bezel overmolded by using a transparent polymer was discussed in this study in order to improve surface quality of the product. Craze criterion was determined by performing mechanical tests for the polymer materials. Craze formation mechanism was revealed by measuring residual stresses of the product, and residual stresses of the product were released by using IR annealing without formation of the craze. Residual stress distribution of the product was also obtained numerically before and after the IR annealing by using three-dimensional flow and structure analyses for the entire overmolding process and IR annealing.

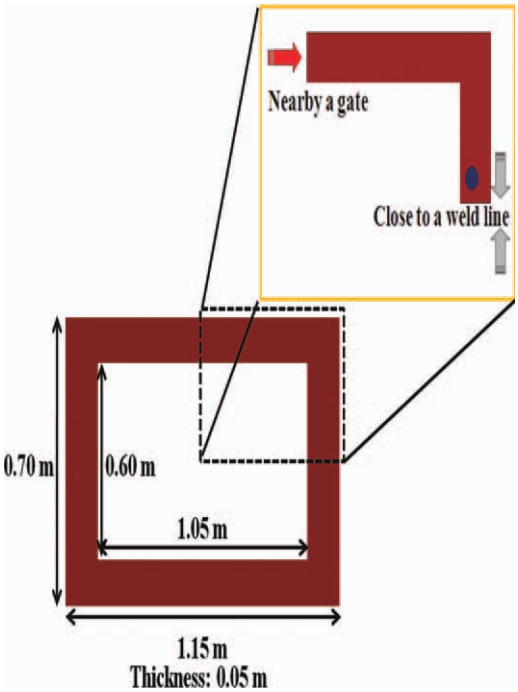

Figure 1 Geometry of the overmolded bezel with the position (blue circle) for measurement of the residual stress distribution by using the hole-drilling method. The experimental and numerical analyses on residual stresses were performed by using the part geometry because of symmetry of the product. [Color figure can be viewed in the online issue, which is available at wileyonlinelibrary.com.]

EXPERIMENTAL

Materials and characterization

PC (Trirex TH3022N, Samyang kasei, Seoul, Korea) was used for the first and second shots of the overmolding. Two kinds of the polymer were employed for molding, that is, transparent and red opaque resins. Those resins were filled with additives over 20 wt % in order to improve flow behavior. The dyes and additives may cause change in mechanical properties of the resins. Tensile tests were performed at room temperature by following the ASTM D638. A universal testing machine (UTM, DEC-MD 5000, Dawha test machine, Bucheon, Korea) was utilized for the tensile test. Bending tests were carried out according to ASTM D790 with the same universal testing machine. For modeling of viscoelastic properties, relaxation moduli of the PC resins were measured by using the dynamic mechanical analysis (DMA 2980, TA Instrument, USA.).

Overmolding and annealing

An injection molding machine (Multiplas Model HM-10T, Taoyuan, Taiwan) with two separate molds was used to prepare the sequentially overmolded TV bezel. Geometry of the TV bezel is shown in Figure 1. At the first stage, a half thickness of the final product was molded by injecting the red PC resin. At the second stage, the opaque PC part was placed as the insert in the second mold that contains extra space for the second shot and the transparent PC resin was injected to form another half of the final product. Processing conditions for the first and second shots are summarized in Table I. The overmolded specimens were annealed at 60°C by surface or IR heating in order to release residual stresses of the specimens.

Measurement of residual stresses

The hole-drilling method was employed to measure residual stresses in the slightly curved TV bezel, since the measurement method had been applied to objects with a small area and a complex geometry. The hole-drilling method is a destructive measurement technique that was first proposed by Mathar.[17] Residual stresses around the hole are released by introduction of a hole at the surface. Removal of stressed material causes localized stress relaxation, and the material around the hole is deformed. Strain distribution induced by the deformation is measured by using a strain gauge as described in the ASTM E837. The experimental set-up and measurement procedure in this study followed the previous study.[4] A three-element strain gage, rosette (062UL type, Measurement Group, USA), was installed on the surface of the overmolded part at the point where residual stresses were to be determined. As

TABLE I
Processing Conditions for the First and Second Shots of the Overmolding

	First shot	Second shot
Melt temperature (°C)	265	265
Injection speed (mm/s)	60	60
Mold temperature (°C)	80	80
Packing pressure (MPa)	8	8
Packing time (s)	10	10
Cooling time (s)	20	20

shown in Figure 1, the rosette was attached to the surface of the product where the residual stress distribution was measured with respect to depth.

A precision milling guide (RS-200, Measurement Group) was placed over the rosette and centered accurately at the drilling target of the rosette. The induced strain at each drilling step was measured and residual stresses were calculated by using the relationship between the strain and principal stress.[18] The integral method was used for measurement of the residual stresses, because the incremental hole-drilling method was appropriate to measure the residual stress distribution in the thickness direction.[20–22]

The elastic strain, ε_{rr}, measured by the rosette at the periphery of the hole, is related to the principal stresses by the following equation.

$$\varepsilon_{rr} = \left(\bar{A} + \bar{B}\cos 2\beta\right)\sigma_{max} + \left(\bar{A} - \bar{B}\cos 2\beta\right)\sigma_{min} \quad (1)$$

$$\bar{A} = -\frac{\bar{a}(1+\nu)}{2E}, \quad \bar{B} = -\frac{\bar{b}}{2E} \quad (2)$$

where σ_{max} and σ_{min} are principal stresses, β is an angle measured counter-clockwise from the maximum principal stress direction to the axis of the strain gage, $\bar{A}$ and $\bar{B}$ are calibration constants, $\bar{a}$ and $\bar{b}$ are dimensionless constants, E is Young's modulus, and ν is Poisson's ratio. Calibration constants were determined by following Ref. 23 and E and ν are listed in Table II. Magnitude and direction of the two principal stresses are obtained in terms of the measured strains.

$$\sigma_{max,}\sigma_{min} = \frac{\varepsilon_1 + \varepsilon_3}{4\bar{A}} \mp \frac{\sqrt{(2\varepsilon_2 - \varepsilon_1 - \varepsilon_3)^2 + (\varepsilon_1 - \varepsilon_3)^2}}{4\bar{B}} \quad (3)$$

$$\beta = \frac{1}{2}\tan^{-1}\left(\frac{2\varepsilon_2 - \varepsilon_1 - \varepsilon_3}{\varepsilon_1 - \varepsilon_3}\right) \quad (4)$$

where ε_1, ε_2, and ε_3 are strains measured by the strain gage.[24]

NUMERICAL SIMULATION

Three-dimensional numerical analysis was used to simulate injection molding steps and predict residual stresses of the part, because the overmolding consists of two shots. Three-dimensional simulation of the injection molding is essential especially for numerical prediction of the viscoelastic deformation of the overmolded product. A mesh generation program, HyperMesh, was used to construct two-dimensional finite elements for two domains for the two shots. Two-dimensional finite elements were created separately for each domain and three-dimensional finite elements were fully generated after they were transported to Moldflow and then combined together.

Flow analysis

The first shot of the overmolding is the same as the filling of the typical injection molding. Governing equations for the flow analysis of the injection molding are the conservation of mass, conservation of momentum, and conservation of energy equations as shown below.[26]

$$\frac{D\rho}{Dt} + \rho(\nabla \cdot v) = 0 \quad (5)$$

$$\rho\frac{Dv}{Dt} = -\nabla P + \nabla \cdot \tau + \rho g \quad (6)$$

$$\rho C_p \frac{DT}{Dt} = \beta T\frac{DP}{Dt} + \eta\dot{\gamma}^2 + \nabla \cdot q \quad (7)$$

where ρ is density, ν is velocity vector, P is pressure, τ is viscous stress tensor, g is gravity vector, C_p is specific heat at constant pressure, β is expansivity, η is generalized Newtonian viscosity, q is heat flux, and $\dot{\gamma}$ is the shear rate.

$$\dot{\gamma} = \sqrt{\left(\frac{\partial u}{\partial z}\right)^2 + \left(\frac{\partial v}{\partial z}\right)^2} \quad (8)$$

where u and v are the velocity components in the x and y directions. The flow front in the cavity is tracked using a fluid concentration equation expressed as below.

TABLE II
Material Properties of the Polycarbonate Employed for Overmolding

Property	PC (Trirex TH3022N)
Elastic modulus (MPa)	2280
Poisson's ratio	0.417
Melt density (kg/m^3)	1123.9
Solid density (kg/m^3)	1252.3
Thermal expansion coefficient (K^{-1})	7.3×10^{-5}
Thermal conductivity (W/m K)	0.297 (at 50°C, temperature-dependent)
Specific heat (J/kg K)	1287 (at 50°C, temperature-dependent)

$$\frac{DF}{Dt} = 0 \tag{9}$$

where F is fluid concentration. Since inserts are treated as a rigid body with no deformation or displacement, mass and momentum conservation in the inserts are ignored.

Three-dimensional flow analysis was performed by assuming that rheological behavior of the polymeric melt satisfies the modified Cross model with the following Williams–Landel–Ferry (WLF) equation.[26]

$$\eta = \frac{\eta_0}{1 + \left(\frac{\eta_0 \dot{\gamma}}{\tau^*}\right)^{(1-n)}}$$
$$\log \frac{\eta_0 \theta^* \rho^*}{\eta^* \theta \rho} = \frac{-C_1(\theta - \theta^*)}{C_2 + (\theta - \theta^*)} \tag{10}$$

where η is viscosity, η_0 is zero shear rate viscosity, $\dot{\gamma}$ is shear rate, t* is shear stress at the transition between Newtonian and power law behavior, η^* is viscosity at reference temperature, ρ is density, ρ^* is density at reference temperature, θ is temperature, and θ^* is reference temperature. Typically, θ^* is chosen as the glass transition temperature and $C_1 = 17.44$ and $C_2 = 51.6$ K for many polymers. Heat conduction through the mold polymer interface, viscous heating during both filling and postfilling stages, and convective heat transfer by the cooling liquid should be considered in the thermal analysis. The modified Tait equation was employed to implement the PVT relationship into the flow simulation. The temperature and flow fields were calculated with the control-volume approach to handle the melt front advancement by applying the hybrid FEM/FDM scheme. An implicit numerical scheme was employed to handle the discretized energy equation.[28]

Residual stresses were calculated by using the hybrid model.[26]

$$\sigma_e^{//} = b_1 \sigma_P + b_2 \tau + b_3$$
$$\sigma_e^{\perp} = b_4 \sigma_P + b_5 \tau + b_6 \tag{11}$$

where $\sigma_e^{\parallel}$ and $\sigma_e^{\perp}$ are the corrected principal stresses in the directions parallel and transverse to flow direction respectively, σ_P is the predicted residual stress, b_i's (where $i = 1,\ldots,6$) are constants to be determined, and τ is a measure of orientation in the material.[26] Heat exchange between the polymer melt and the previously molded part that is recognized as an insert must be evaluated during the second shot. Since the energy balance must be taken into account in the second shot, the energy equation for the cavity given in eq. (7) can be simplified for the insert as below[26] by assuming that the insert is a rigid body.

$$\rho C_p \frac{\partial T}{\partial t} = \nabla \cdot q \tag{12}$$

Properties of a PC resin (Trirex TH3022N, Samyang kasei) were chosen as the properties of the injected resin for flow analyses of the two shots. Selected material properties are summarized in Table II. Molding conditions for the numerical predictions are the same as the experimental conditions in Table I. At the end of the flow analysis, the output data were exported to the stress analysis program and the interface between the two parts was joined by assuming perfect interface bonding. The in-mold stress condition of the overmolded part was exported to the stress simulation code, ABAQUS, and used as the initial condition for structural analysis of the overmolded product.

Stress analysis

Residual stress distribution and deformation of the overmolded parts were predicted by applying elastic properties of the solid polymer. However, it is well known that viscoelastic properties are considered to predict time-dependent deformation of polymeric solid parts that are exposed to environmental conditions. For prediction of long-term viscoelastic deformation of the polymeric part, it was assumed that the viscoelastic polymer was isotropic and the temperature effect on material behavior was explained by the thermo-rheological simplification. Constitutive equation of the generalized Kelvin model was selected as that of the linear thermoviscoelastic material. The linear thermoviscoelastic constitutive equation is represented by hereditary integrals and the temperature effect is considered by the following equation.[29]

$$\tau(t) = G_0(\theta)\left(\gamma - \int_0^t \dot{g}_R(\xi(s))\gamma(t-s)ds\right) \tag{13}$$

where the instantaneous shear modulus G_0 is temperature-dependent and γ is the shear strain.

$$\dot{g}_R(\xi) = dg_R/d\xi$$
$$g_R(t) = G_R/G_0 \tag{14}$$

where $G_R(t)$ is the shear relaxation modulus that characterizes the material's response as a function of time and $g_R(t)$ is dimensionless relaxation modulus. $\xi(t)$ is the reduced time defined by the following equation.

$$\xi(t) = \int_0^t \frac{ds}{A(\theta(s))} \tag{15}$$

where $A(\theta(t))$ is a shift function at time t. Temperature dependence of the reduced time is usually referred to as the thermo-rheologically simple temperature

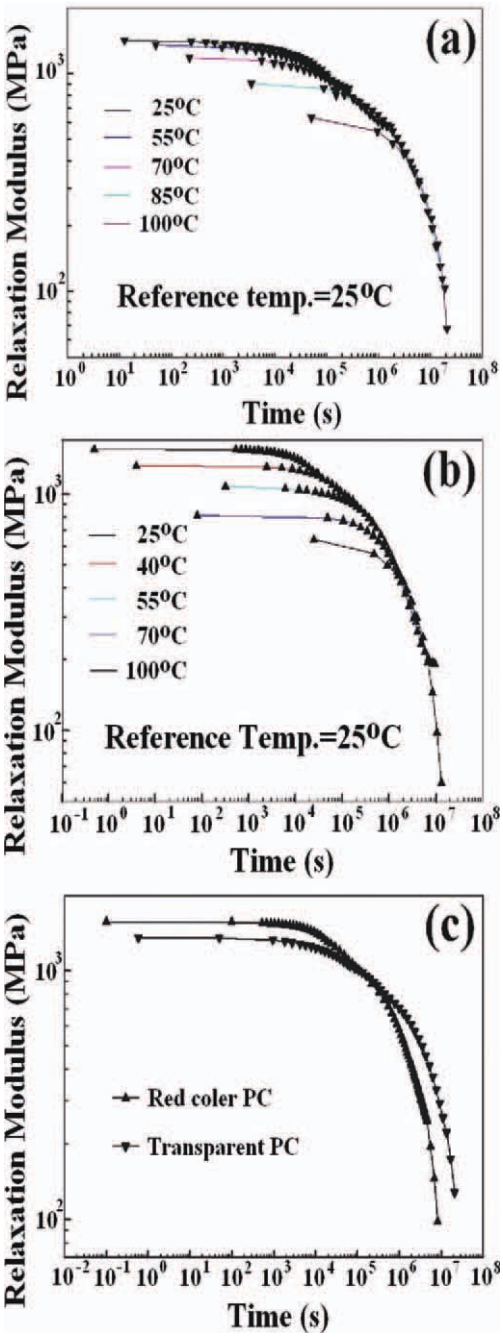

Figure 2 Relaxation moduli for thermoviscoelastic analysis: (a) the colorless transparent PC for the second shot, (b) the red PC for the first shot, and (c) master curves of the two kinds of PCs. [Color figure can be viewed in the online issue, which is available at wileyonlinelibrary.com.]

dependence. The shift function is often approximated by the WLF form.

$$\log(A) = \log\left(\frac{t}{t_0}\right) = \frac{-C_1'(\theta - \theta^*)}{C_2' + (\theta - \theta^*)} \tag{16}$$

where θ* is the reference temperature at which the relaxation data are provided and C_1' and C_2' are calibration constants obtained at the temperature.

$$C_1' = \frac{C_1^g}{1 + (\theta^* - \theta_g)/C_2^g}, \quad C_2' = C_2^g + \theta^* - \theta_g \tag{17}$$

where C_1^g and C_2^g are universal constants, which are 17.4 and 51.6 K, respectively.

Normalized relaxation moduli of the two parts were measured as shown in Figure 2 and used for the isotropic viscoelastic stress analysis. The relaxation moduli were measured for the temperature varying from 25 to 100°C, and the master curve was constructed by applying the shift function.[31] The ejection step was established by solving an elastic problem when fixed boundary conditions are eliminated suddenly and the thermal annealing step was dealt with by assuming that the part was kept at 60°C for 30 min. IR annealing step was treated by applying radiation heat transfer and using emissivity coefficients as shown in Figure 3. The used emissivity coefficients of the PC for the first and second shots were 0.2 and 0.95, respectively.

RESULTS AND DISCUSSION

Crazes are created from stress-concentrated nuclei such as micro voids, stretched chains, and dusts. Crazes, which are irreversible and permanent, occur

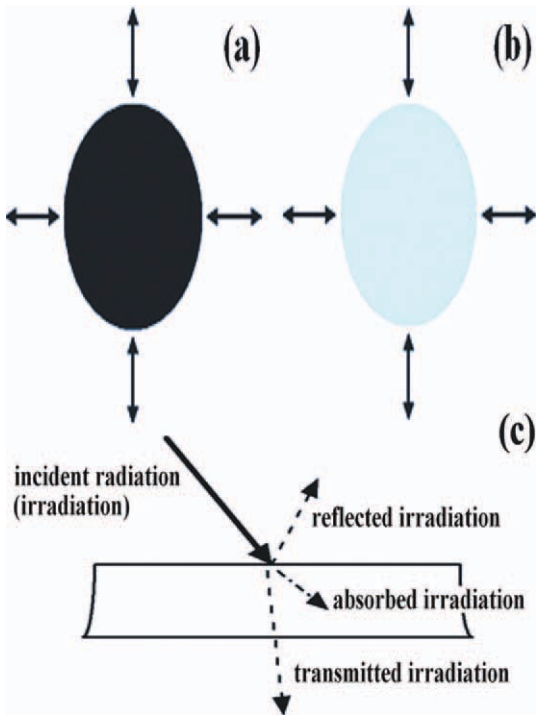

Figure 3 Schematic diagrams for emissivity of black and gray bodies for ABAQUS analysis of the IR annealing with radiation heat transfer: (a) black body (emissivity coefficient, $\varepsilon = 1$), (b) gray body (emissivity coefficient, $0 < \varepsilon < 1$), and (c) reflected, absorbed, and transmitted radiation. [Color figure can be viewed in the online issue, which is available at wileyonlinelibrary.com.]

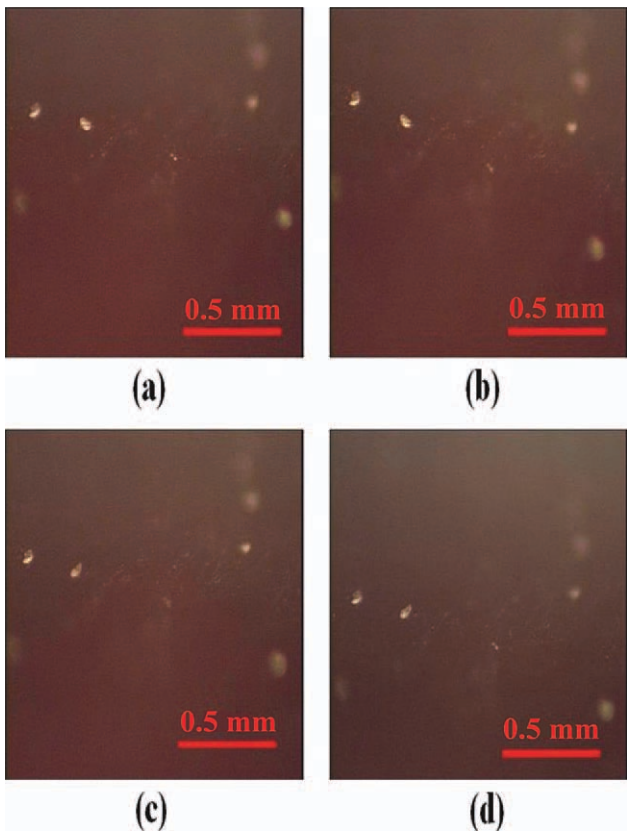

Figure 4 Observation of micro voids as a function of annealing time after thermal annealing of the overmolded product: (a) unannealed (initial state after ejection), (b) annealed at 60°C for 5 min, (c) annealed at 60°C for 10 min, and (d) annealed at 60°C for 30 min. [Color figure can be viewed in the online issue, which is available at wileyonlinelibrary.com.]

in the perpendicular direction to the maximum principal stresses.[32] It was observed that defects or micro voids generated at the interface between the different PC's molded by the two shots acted as the nuclei for crazing. Micro voids were observed before and after annealing at 60°C for 5–30 min as shown in Figure 4. However, there was no change after each annealing condition, which indicated that the micro voids did not act as the nuclei for crazing during thermal annealing. In contrast, crazes were observed at the region slightly adjacent to the micro void and near the interface after the thermal annealing at 60°C for 10 min as shown in Figure 5. More crazing was observed as the annealing time was increased, but cracks were not observed. These results implied that crazes were generated during thermal annealing due to stress concentration near the region adjacent to the micro voids and the interface.

Previous study suggested stress criterions for craze and crack formation in transparent amorphous polymers.[32] Temperature effects on craze formation and dependence of the craze criterion on temperature were studied.[33] The craze criterion was lowered when the temperature rose, indicating easier formation of craze at high temperature. Stress criterion for craze formation was determined by performing a tensile test in this study as displayed in Figures 6 and 7. The craze was not observed at room temperature irrespective of tensile stress and direct crack initiation was observed in the case of the notched tensile test specimen. Stress limit for crazing of the used PC was illustrated in Figure 6 with respect to temperature. Crazing was not observed at room temperature but they were generated at 60 and 80°C when the applied tensile stress was larger than 20 MPa as shown in Figure 7. Therefore, residual stress of the injection-molded part should be lower than 20 MPa in order to prevent crazing of the transparent PC. As shown by the bending test result in Figure 8, crazing was observed at room temperature but crack formation did not occur under the applied stress of 100 MPa that was bending strength of the material, because crazes were formed at lower stress than cracks.[32]

Residual stress distribution was measured in the thickness direction by using the incremental

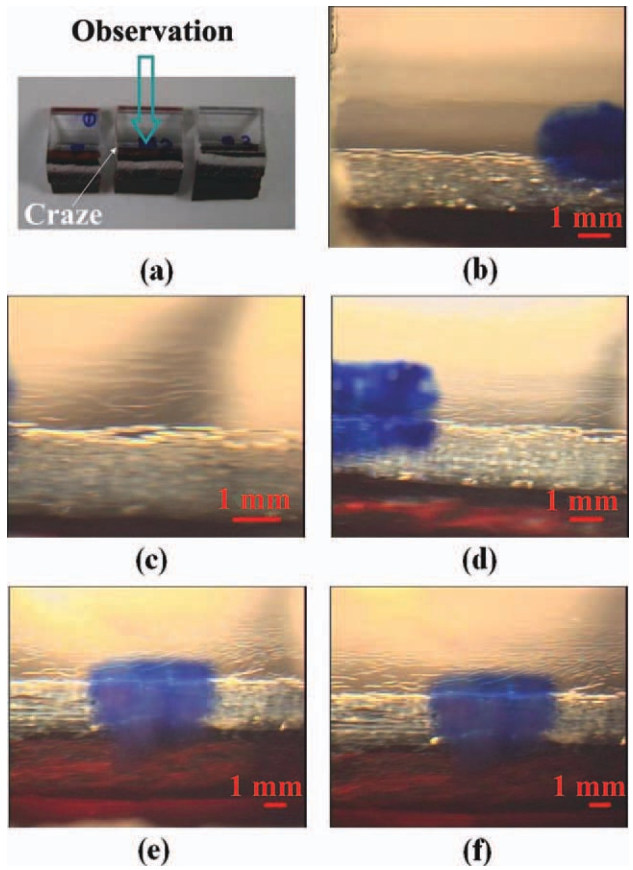

Figure 5 Observation of craze formation near the interface region as a function of thermal annealing time: (a) observation direction, (b) unannealed (initial state; at ejection), (c) annealed at 60°C for 10 min, (d) annealed at 60°C for 30 min, (e) annealed at 80°C for 10 min, and (f) annealed at 80°C for 30 min. [Color figure can be viewed in the online issue, which is available at wileyonlinelibrary.com.]

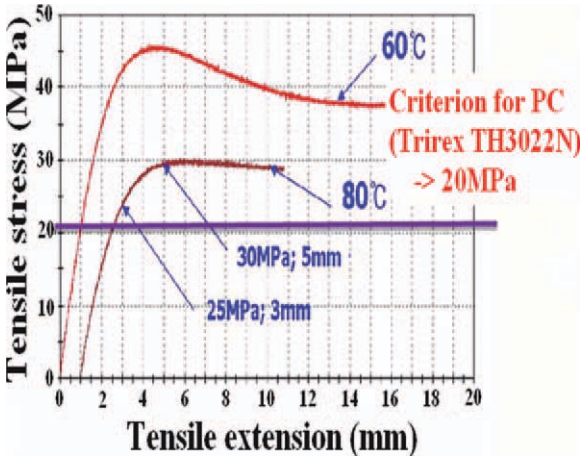

Figure 6 The craze stress criterion determined by the tensile test at different temperature for the PC (Trirex TH3022N). The determined craze criterion was 20 MPa when the temperature was over 60°C. [Color figure can be viewed in the online issue, which is available at wileyonlinelibrary.com.]

hole-drilling method as shown in Figure 9. The blind hole was drilled from the surface by 10 times to make a hole of 2-mm depth. The residual stress distribution in the overmolded specimen was altered after the IR annealing and the stress values were totally lowered when compared with the unannealed specimen. Qualitative estimation of residual stresses

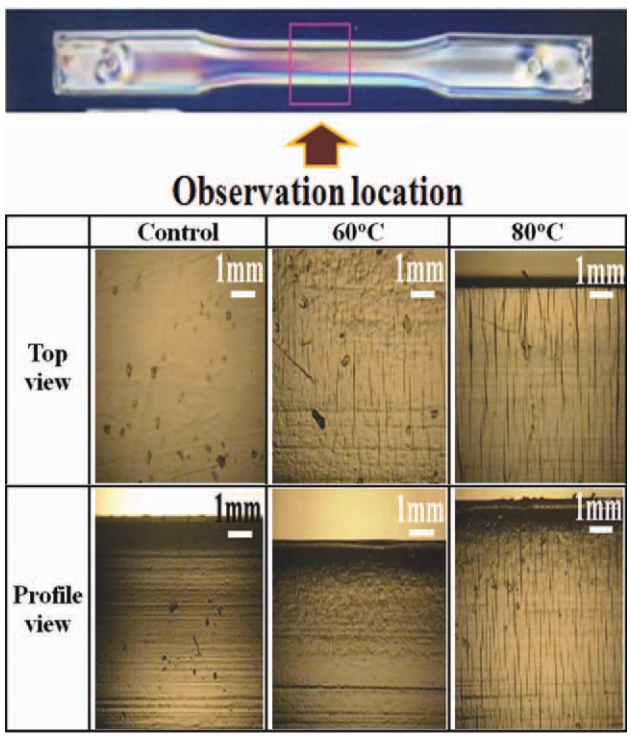

Figure 7 Top and profile view for craze formation of the PC (Trirex TH3022N) during tensile test at different temperature. [Color figure can be viewed in the online issue, which is available at wileyonlinelibrary.com.]

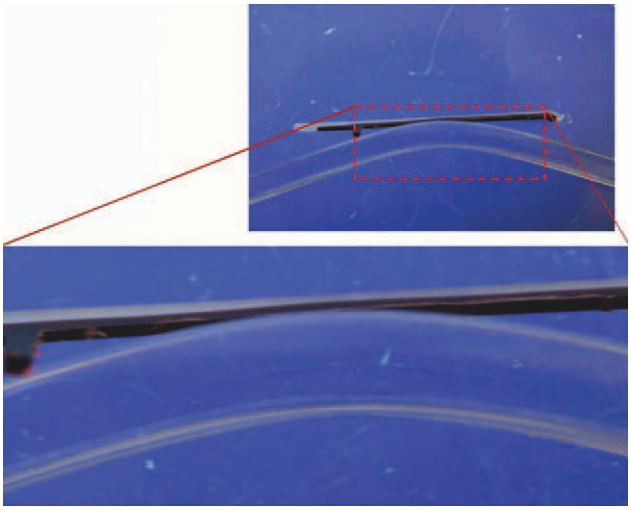

Figure 8 Craze formation of the PC (Trirex TH3022N) after bending test. [Color figure can be viewed in the online issue, which is available at wileyonlinelibrary.com.]

in the injection-molded part is possible by using the birefringence measurement. Residual stresses of the unannealed specimen were higher than those of the IR annealed specimen near the weld line as shown in Figure 10. Since external impact force and high temperature can impose critical influence on deformation or failure of injection-molded parts with high residual stresses, annealing process should be applied to the injection-molded parts for relaxation of the residual stresses.

The part geometry and residual stress results of the flow analysis were exported to the structural analysis program in order to perform thermoviscoelastic stress analysis aforementioned. Residual stresses of both the ejected and IR annealed products

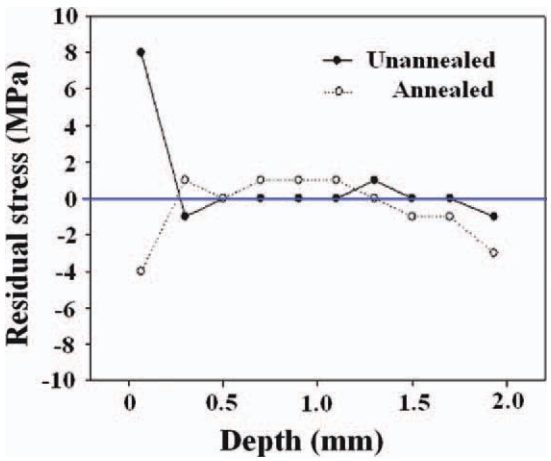

Figure 9 Residual stresses distribution measured by the hole-drilling method at the position shown in Figure 1 near the interface between the first and second shots: (a) unannealed and (b) IR annealed. [Color figure can be viewed in the online issue, which is available at wileyonlinelibrary.com.]

are shown in Figure 11. Crazes are expected if the temperature is higher than 60°C and the tensile residual stress is higher than 20 MPa as discussed above. Residual stresses over 20 MPa are observed widely in Figure 11(a) but residual stresses are lower than 20 MPa in most regions as shown in Figure 11(b), indicating that residual stresses were released significantly by the IR annealing. The numerically predicted residual stresses were in good agreement with the experimental results as shown in Figure 9. Therefore, it is concluded that overmolding process, thermoviscoelastic behavior of the transparent polymer, and IR annealing process were modeled properly by the three-dimensional numerical simulations.

CONCLUSIONS

Crazes are created by stress concentration at nuclei such as micro voids, stretched chains, and dusts. Cracks are formed from the crazes as more stresses are accumulated. Cracks can appear suddenly without craze formation in some cases depending upon mechanical and thermal characteristics of the polymeric materials. Craze generation in a product overmolded with a transparent polymer was discussed in this study in order to improve optical quality of the product. Craze criterion was determined at the temperature over 60°C by using mechanical analysis of the injection-molded polymeric material. Residual stresses of the molded product were higher than 20 MPa after ejection, but crazes were not created at room temperature. Crazes were observed in the overmolded product annealed at over 60°C due to thermal residual stresses caused by the temperature difference between the surface and inside of the product upon surface heating. However, crazes were not observed in the overmolded product annealed by IR heating due to simultaneous heating at both the surface and inside of the part. Residual stresses obtained by the numerical prediction were in good agreement with the experimental results. Overmolding process, thermoviscoelastic property of polymeric materials, and IR annealing process were modeled properly by the three-dimensional numerical analysis.

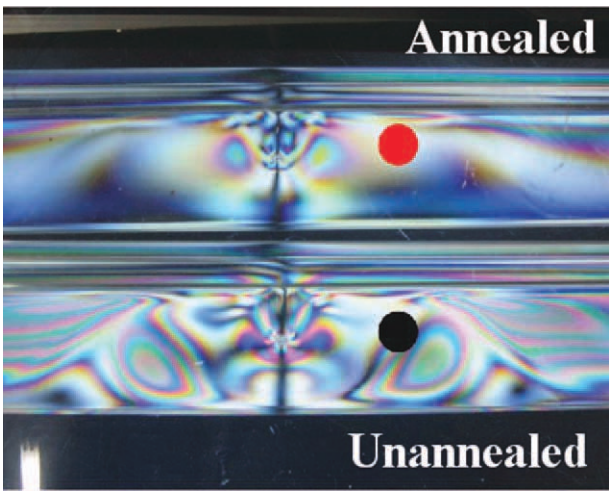

Figure 10 Residual stresses of the unannealed and IR annealed specimens near the weld line. The spots were the positions where the residual stress distribution was measured. [Color figure can be viewed in the online issue, which is available at wileyonlinelibrary.com.]

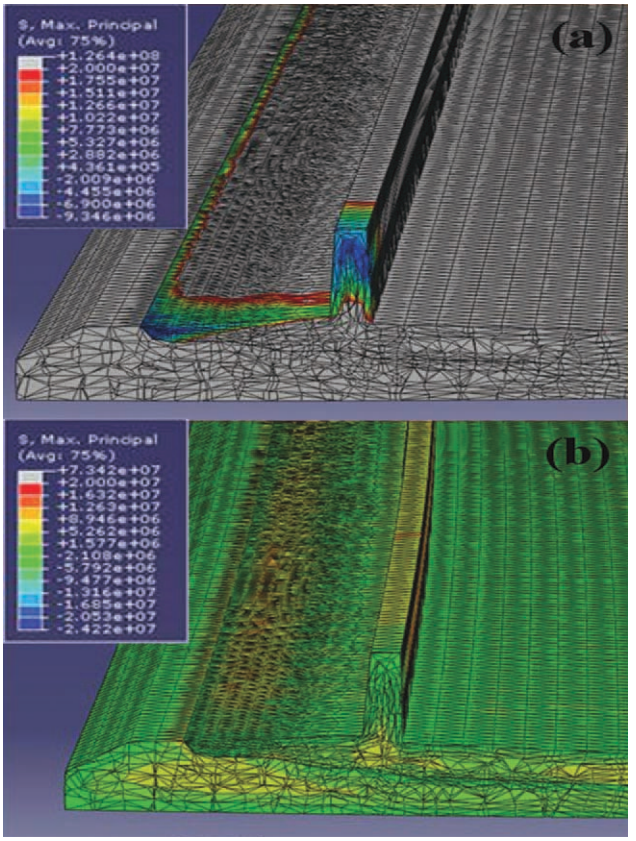

Figure 11 Maximum principal stresses in the part: (a) initial state and (b) after the IR-annealing. Contour limitation was set at 20 MPa at room temperature. [Color figure can be viewed in the online issue, which is available at wileyonlinelibrary.com.]

References

1. Isayev, A. I.; Crouthamel, D. L. Polym Plast Technol Eng 1984, 22, 177.
2. Haworth, B.; Hindle, C. S.; Sandilands, G. J.; White, J. R. Plast Rubber Proc Appl 1982, 2, 59.
3. Kim, S. Y.; Lee, J. T.; Kim, J. Y.; Youn, J. R. Polym Eng Sci 2010, 50, 1205.
4. Kim, S. Y.; Kim, C. H.; Kim, S. H.; Oh, H. J.; Youn, J. R. Polym Test 2009, 28, 500.
5. Kim, S. Y.; Oh, H. J.; Kim, S. H.; Kim, C. H.; Lee, S. H.; Youn, J. R. Polym Eng Sci 2008, 48, 1840.
6. Zhang, X.; Cheng, X.; Stelson, K. A.; Bhattacharya, M.; Sen, A.; Voller, V. R. J Therm Stress 2002, 25, 523.
7. Sen, A.; Bhattacharya, M. Polymer 2000, 41, 9177.
8. Coxon, L. D.; White, J. R. Polym Eng Sci 1980, 20, 230.
9. Sperling, L. H. Introduction to Physical Polymer Science; Wiley: New York, 2001.

10. Dondero, M.; Pastor, J. M.; Carella, J. M.; Perez, C. J. Polym Eng Sci 2009, 49, 1886.
11. Arzondo, L. M.; Pino, N.; Carella, J. M.; Pastor, J. M.; Merino, J. C.; Póveda, J.; Alonso, C. Polym Eng Sci 2004, 44, 2110.
12. Kim, S. Y.; Kim, S. H.; Oh, H. J.; Lee, S. H.; Youn, J. R. J Appl Polym Sci 2010, 118, 2530.
13. Kim, S. Y.; Lee, S. H.; Youn, J. R. Int Polym Proc 2010, 25, 109.
14. Kim, S. Y.; Kim, S. H.; Oh, H. J.; Lee, S. H.; Baek, S. J.; Youn, J. R.; Lee, S. H.; Kim, S.-W. J Appl Polym Sci 2009, 111, 642.
15. Kim, S. Y.; Lee, S. H.; Baek, S. J.; Youn, J. R. Macromol Mater Eng 2008, 293, 969.
16. Kim, S. Y.; Kim, S. H.; Kim, J. Y.; Cho, H. H. J Appl Polym Sci 2007, 104, 205.
17. Mathar, J. Iron Steel 1934, 56, 249.
18. ASTM International. Determining Residual Stresses by the Hole-Drilling Strain-Gage Method, Annual Book of ASTM E837-01; ASTM International: West Conshohocken, 2001.
19. Measurement Group. Measurement of Residual Stresses by the Hole-Drilling Strain Gage Method, Tech Note TN-503-5; Measurement Group: North Carolina, 1993.
20. Wang, T.; Young, W. Eur Polym J 2005, 41, 2511.
21. Maxwell, A. S.; Turnbull, A. Polym Test 2003, 22, 231.
22. Sicot, O.; Gong, X. L.; Cherouat, A.; Lu, J. J Compos Mater 2003, 37, 831.
23. Kim, C. H.; Youn, J. R. Polym Test 2007, 26, 862.
24. Schajer, G. S. J Eng Mater Trans ASME 1988, 110, 338.
25. Flaman, M. T.; Manning, B. H. Exp Mech 1985, 25, 205.
26. Kennedy, P. Flow Analysis Reference Manual; Moldflow: Kilsyth, Australia, 1993.
27. Macosko, C. W. Rheology, Principles, Measurements, and Applications; Wiley-VCH: New York, 1994.
28. Santhanam, N.; Chiang, H. H.; Himasekhar, K.; Tuschak, P.; Wang, K. K. Adv Polym Technol 1991, 11, 77.
29. ABAQUS. Analysis User's Manual; ABAQUS: Rhode Island, 2003; Vol.3.
30. Flügge, W. Viscoelasticity; Springer-Verlag: New York, 1975.
31. Stefano, T.; Roberto, V.; Marinella, L.; Marco, C.; Aldo, S. Eur Polym J 2008, 44, 2951.
32. Bucknall, C. B. Polymer 2007, 48, 1030.
33. Oxborough, R. J.; Bowen, P. B. Philos Mag 1973, 28, 547.